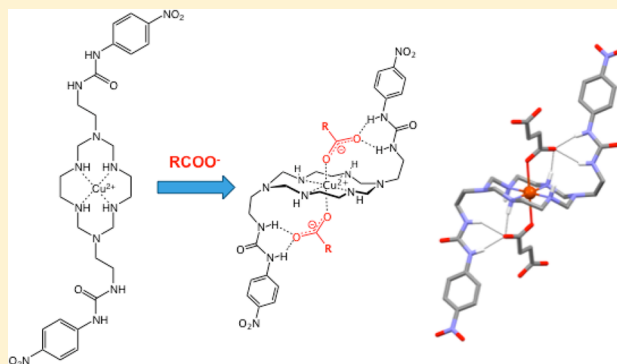


Oxo-Anion Recognition by Mono- and Bisurea Pendant-Arm Macrocyclic Complexes

Massimo Boiocchi,[†] Maurizio Licchelli,^{*,‡} Michele Milani,[‡] Antonio Poggi,[‡] and Donatella Sacchi[‡][†]Centro Grandi Strumenti and [‡]Dipartimento di Chimica, Università di Pavia, via T. Taramelli 12, 27100 Pavia, Italy

S Supporting Information

ABSTRACT: The novel macrocyclic copper(II) complexes [2]²⁺ and [3]²⁺, carrying one or two (nitrophenyl)urea fragments appended to an azacyclam or diazacyclam framework, exploit the hydrogen-bond-forming abilities of the urea subunits, along with the metal–ligand interaction, in the recognition of anionic species. Equilibrium studies in acetonitrile performed on [2]²⁺ and [3]²⁺ show that (nitrophenyl)urea pendant arms strongly interact with anionic species such as carboxylates and phosphates, which display both coordinating tendencies toward copper(II) and good affinity toward urea subunits. Stability constants of the adducts are considerably higher than those determined for the interaction of the same anions with a “plain urea” reference compound, confirming the synergistic action of metallomacrocyclic and urea subunits. Complex [2]²⁺ forms 1:1 adducts with acetate, benzoate, hydrogendiphosphate, and dihydrogen phosphate, while complex [3]²⁺ interacts with the same anions according to both 1:1 and 1:2 stoichiometries, with the exception of hydrogendiphosphate, which forms only the 1:1 adduct with a distinctly high association constant (log *K* > 7). Spectrophotometric investigations suggest that oxoanionic species interact with the complexes according to a “bridged” mode, inducing the macrocyclic systems to adopt a scorpionate-like conformation, as confirmed by crystallographic studies on the [3]²⁺/succinate adduct.



■ INTRODUCTION

Molecular recognition of anionic species has attracted increasing interest during the last decades^{1–3} because of the important role played by anions in biological and environmental processes.^{2,4,5} A very large number of artificial systems for recognition and sensing of anions have been designed and synthesized by properly exploiting supramolecular concepts.^{6–12}

Recognition of anionic species is often accomplished by electrostatic and/or hydrogen-bonding interactions. In their pioneering work, Lehn and Schmidtchen^{13,14} developed positively charged cagelike receptors able to incorporate inorganic anions. In these kinds of receptors, selectivity is mainly based on the matching of the geometrical features (shape and size) of both the anion and the host's cavity. Hydrogen bonding, despite its fundamentally electrostatic nature, has a directional character and, in principle, allows better discrimination between anions with different structural and electronic features than genuine electrostatic interactions.¹⁵ Therefore, a variety of molecular receptors have been developed that perform recognition of their anionic targets by establishing a complementary set of hydrogen bonds.^{8,16–19} Some classes of compounds, for instance, cyclic and acyclic polyammonium receptors, interact with anions by combining pure electrostatic and hydrogen-bonding interactions.^{20–23}

Among hydrogen-bonding donor groups, urea and thiourea have been frequently employed as anion binding fragments. In fact, they are able to form two hydrogen bonds in a parallel fashion, displaying an enhanced complementarity toward Y-shaped oxo anions (e.g., carboxylates). Seminal papers by Wilcox and Hamilton^{24,25} showed the excellent anion complexation properties displayed by urea-containing molecular receptors. Since then, a large number of receptors and sensors containing one or more urea/thiourea units in their structure have been reported.^{26–33}

A large number of anion receptors based on metal centers have also been reported.^{34–38} In these systems, metal ions can play a merely structure-organizing role or be directly involved in the anion binding. In the first case, for instance, the coordination of properly functionalized ligand(s) around a metal ion can result in the formation of a highly organized system displaying one or more sites suitable for anion binding through electrostatic or hydrogen-bonding interactions.^{34,35} In the second case, metal–ligand interactions are directly involved in anion binding and recognition, exploiting the definite coordinating tendencies of this kind of substrate toward metal ions.^{36–38} Coordinative interactions are usually stronger than electrostatic interactions (including the hydrogen bond);

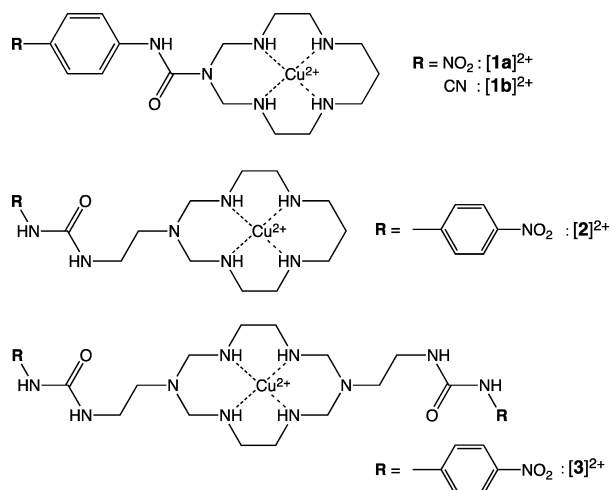
Received: June 27, 2014

Published: December 22, 2014



moreover, they display a more definite directional character and may impose further geometrical constraints, which contribute to increasing selectivity in the recognition process. A metal–ligand subunit included in the structure of an anion receptor should be coordinatively unsaturated, thus leaving one (or more) binding site(s) available for the anionic substrate, and should establish with it kinetically labile interactions to provide a fast and reversible interaction (as requested for the recognition process). On the other hand, metal centers should be firmly retained in the receptor structure in order to prevent release of the metal ion and loss of the anion binding ability. Macrocyclic complexes fulfill these requirements because (i) they are usually characterized by high thermodynamic stability and are kinetically inert^{39–41} and (ii) they may interact at the axial position(s) with additional ligand(s) and this interaction is kinetically labile.

In spite of the large number of examples concerning anion recognition processes based on either hydrogen bonds or coordinative interactions, a relatively small number of synthetic receptors have been reported, which exploit both interactions at the same time.^{42,43} In particular, a few years ago we reported the synthesis and solution behavior of a couple of receptors for anions characterized by a macrocyclic complex framework.⁴⁴ Copper complexes $[1a]^{2+}$ and $[1b]^{2+}$ incorporating a urea subunit are able to recognize oxo anions exploiting the cooperative effect because of the proximity of a coordinatively unsaturated metal center and a hydrogen-bonding donor group. It should be noted that compounds $[1a]^{2+}$ and $[1b]^{2+}$ were obtained by a template reaction in which ureas were used as “locking fragments”;^{41,45} therefore, a nitrogen of the urea group is incorporated into the macrocyclic azacyclam framework. This prevents full exploitation of the tendencies of urea moieties to form several hydrogen bonds at the same time (in particular toward Y-shaped anions).



We report here the synthesis of two novel macrocyclic compounds, $[2]^{2+}$ and $[3]^{2+}$, in which one or two genuine urea fragments are appended onto an azacyclam or diazacyclam structure, respectively. In principle, these compounds could fully exploit the hydrogen-bond-forming abilities of urea subunits, along with the metal–ligand interaction, in the recognition process. Equilibrium studies in acetonitrile (MeCN) performed on $[2]^{2+}$, $[3]^{2+}$, and “plain urea” reference compound **6** have shown that (nitrophenyl)urea pendant arm(s) strongly interact with carboxylate and phosphate anions and that the proximate copper(II) macrocycle subunit

considerably increases their binding ability toward the oxo anions.

EXPERIMENTAL SECTION

General Procedures and Materials. All reagents for syntheses were purchased from Sigma-Aldrich and used without further purification.

N-tert-Butoxycarbonyldiaminoethane, en-BOC, was prepared according to the literature.⁴⁶ The copper complex of 1,8-bis(2-aminoethyl)-1,3,6,8,10,13-esazacyclotetradecane was prepared according to the literature method and isolated as the diammonium tetraperchlorate salt $[5](\text{ClO}_4)_4$.⁴⁷

Carbon, hydrogen, and nitrogen elemental analyses were carried out using a Costech ECS 4010 instrument at the Department of Chemistry, Materials, and Chemical Engineering “G. Natta”, Politecnico di Milano, Milan, Italy. ^1H and ^{13}C NMR spectra were acquired on a Bruker Avance 400 spectrometer. Mass spectrometry (MS) spectra were acquired using a Thermo-Finnigan ion trap LCQ Advantage Max instrument equipped with an electrospray ionization (ESI) source. IR spectra were run on a PerkinElmer Spectrum X100 Fourier transform infrared (FT-IR) instrument equipped with an attenuated total reflectance (U-ATR) apparatus. UV–vis spectra were recorded using a Varian Cary 50 or Cary 100 spectrophotometer with a quartz cuvette (path length: 1 or 0.1 cm).

All titrations were performed at 25 °C on solutions of $[2](\text{ClO}_4)_2$ and $[3](\text{ClO}_4)_2$ in MeCN. Aliquots of freshly prepared standard solutions of $[\text{Bu}_4\text{N}]\text{X}$ ($\text{X} = \text{CH}_3\text{COO}^-$, $\text{C}_6\text{H}_5\text{COO}^-$, NO_3^- , H_2PO_4^- , and HSO_4^-) and $[\text{Bu}_4\text{N}]\text{HP}_2\text{O}_7$ in MeCN were added, and a UV–vis spectrum of the resulting solution was taken after every addition. Spectral intensities were corrected for the dilution factor. Solutions of succinate and glutarate in MeCN were prepared by the addition of stoichiometric amounts of $[\text{Et}_4\text{N}]\text{OH}$ to solutions of the corresponding dicarboxylic acid. Titration data were processed with the *Hyperquad* software package⁴⁸ to determine the equilibrium constants. Care was taken that in each titration the *p* parameter ($p = [\text{concentration of complex}]/[\text{maximum possible concentration of complex}]$) was lower than 0.8, a condition required for the safe determination of a reliable equilibrium constant.⁴⁹

Safety note! Perchlorate salts of metal complexes are potentially explosive and should be handled with care. In particular, they should never be heated as solids.⁵⁰

Synthesis of $[4](\text{ClO}_4)_3$. *N,N'*-Bis(2-aminoethyl)propane-1,3-diamine (2,3,2-tet; 0.4 g, 2.5 mmol), en-BOC (0.4 g, 2.5 mmol), 36.5% aqueous formaldehyde (2.0 mL, 26.5 mmol), and triethylamine (0.75 mL, 5.4 mmol) were added to a solution of $\text{Cu}(\text{CH}_3\text{COO})_2 \cdot \text{H}_2\text{O}$ in methanol (50 mL). The resulting mixture was magnetically stirred and heated at reflux for 24 h. After cooling at room temperature, 65% aqueous HClO_4 (20 mL) was added and a pink solid precipitated. It was recovered by filtration and recrystallized from 0.1 M aqueous HClO_4 . Yield: 30%. Anal. Calcd for $\text{C}_{11}\text{H}_{29}\text{Cl}_3\text{CuN}_6\text{O}_{12}$ (607.3): C, 21.8; H, 4.8; N, 13.8. Found: C, 21.5; H, 4.6; N, 13.6. ESI-MS (MeCN): m/z 508 (100%; $[\text{M} - \text{ClO}_4]^{+}$). FT-IR (solid, ATR): 3525 (m), 3247 (m), 3180 (m), 2970 (w), 2888 (w), 1602 (m), 1504 (m), 1472 (m), 1428 (m), 1052 (vs), 998 (s), 620 (s) cm^{-1} . UV–vis [H_2O ; λ_{max} nm (ϵ , $\text{M}^{-1} \text{cm}^{-1}$): 500 (67).

Synthesis of $[2](\text{ClO}_4)_2$. A solution of (4-nitrophenyl)isocyanate (0.27 g, 1.65 mmol) in anhydrous MeCN (20 mL) was added dropwise under a dinitrogen atmosphere to a round-bottomed flask containing a solution of $[4](\text{ClO}_4)_3$ (1 g, 1.65 mmol), triethylamine (0.92 mL, 6.6 mmol), and pyridine (0.53 mL, 6.6 mmol) in anhydrous MeCN (30 mL). The resulting mixture was magnetically stirred at room temperature for 5 h. The pink solid that precipitated during the reaction was isolated by filtration, washed with cold MeCN (10 mL), and dried in vacuo. Yield: 71%. Anal. Calcd for $\text{C}_{18}\text{H}_{32}\text{Cl}_2\text{CuN}_8\text{O}_{11}$ (670.9): C, 32.2; H, 4.8; N, 16.7. Found: C, 32.4; H, 4.9; N, 16.5. ESI-MS (MeCN): m/z 572 (100%; $[\text{M} - \text{ClO}_4]^{+}$), 235 (25%; $[\text{M} - 2\text{ClO}_4]^{2+}$). FT-IR (solid, ATR): 3425 (w), 3388 (m), 3230 (m), 2951 (w), 2887 (w), 1700 (s), 1655 (w), 1608 (m), 1594 (m), 1534

(s), 1505 (s), 1485 (s), 1446 (m), 1425 (m), 1365 (w), 1316 (vs), 1295 (s), 1207 (s), 1170 (m), 1154 (m), 1104 (s), 1081 (s), 1071 (s), 1054 (vs), 997 (s), 954 (s), 876 (m), 838 (m), 743 (m), 684 (m), 616 (s) cm^{-1} . UV-vis [CH_3CN ; λ_{max} nm (ϵ , $\text{M}^{-1} \text{cm}^{-1}$): 335 (17050), 501 (68).

Synthesis of $[3](\text{ClO}_4)_2$. $[5](\text{ClO}_4)_4$ (1.00 g, 1.33 mmol) was dissolved in anhydrous MeCN (30 mL) under a dinitrogen atmosphere, and then triethylamine (0.74 mL, 5.32 mmol) and pyridine (0.43 mL, 5.32 mmol) were added to the mixture. A solution of (4-nitrophenyl)isocyanate (0.44 g, 2.66 mmol) in anhydrous MeCN (20 mL) was slowly added, and the resulting mixture was stirred for 5 h at room temperature. A pink precipitate was filtered off, washed with cold MeCN (10 mL), and dried in vacuo. Yield: 80%. Anal. Calcd for $\text{C}_{26}\text{H}_{40}\text{Cl}_2\text{CuN}_{12}\text{O}_{14}$ (879.1): C, 35.5; H, 4.6; N, 19.1. Found: C, 35.5; H, 4.7; N, 19.2. ESI-MS (MeOH): m/z 780 (50%; $[\text{M} - \text{ClO}_4]^+$), 340 (100%; $[\text{M} - 2\text{ClO}_4]^{2+}$). FT-IR (solid, ATR): 3433 (w), 3394 (m), 3235 (m), 2952 (w), 2885 (w), 1705 (s), 1661 (w), 1613 (m), 1600 (m), 1542 (s), 1510 (s), 1490 (s), 1456 (m), 1431 (m), 1374 (w), 1325 (vs), 1301 (s), 1272 (m), 1213 (s), 1176 (m), 1159 (m), 1109 (s), 1090 (s), 1075 (s), 1059 (vs), 1000 (s), 960 (s), 932 (w), 883 (m), 843 (m), 749 (m), 688 (m), 619 (s) cm^{-1} . UV-vis [CH_3CN ; λ_{max} nm (ϵ , $\text{M}^{-1} \text{cm}^{-1}$): 336 (32800), 498 (69).

Synthesis of *N*-(4-Nitrophenyl)-*N'*-propylurea (6). A solution of (4-nitrophenyl)isocyanate (0.22 g, 1.33 mmol) in anhydrous MeCN (20 mL) was slowly added under a dinitrogen atmosphere to a solution containing propylamine (0.078 g, 1.33 mmol), triethylamine (0.37 mL, 2.66 mmol), and pyridine (0.21 mL, 2.66 mmol) in anhydrous MeCN (10 mL). After 5 h of magnetic stirring, a yellow precipitate formed. It was separated by filtration, washed with MeCN, and dried in vacuo. Yield: 82%. ESI-MS: m/z 222 (100%; $[\text{M} - \text{H}]^+$). ^1H NMR [400 MHz, dimethyl sulfoxide ($\text{DMSO}-d_6$, 25 $^\circ\text{C}$): δ 0.88 (t, 3H, CH_3), 1.45 (m, 2H, CH_2), 3.06 (m, 2H, CH_2), 6.45 (m, 1H, NH), 7.62 (d, 2H, arom), 8.15 (d, 2H, arom), 9.23 (d, 1H, NH). ^{13}C NMR (100 MHz, $\text{DMSO}-d_6$, 25 $^\circ\text{C}$): δ 12.12 (s, 1C, CH_3), 23.61 (s, 1C, CH_2), 41.78 (s, 1C, CH_2), 117.61 (s, 2C, arom), 125.98 (s, 2C, arom), 141.18 (s, 1C, arom), 148.10 (s, 1C, arom), 155.23 (s, 1C, CO). UV-vis [CH_3CN ; λ_{max} nm (ϵ , $\text{M}^{-1} \text{cm}^{-1}$): 336 (16200).

X-ray Crystallographic Studies. Diffraction data for $[3](\text{ClO}_4)_2$ (red, $0.35 \times 0.22 \times 0.12 \text{ mm}^3$) and $[3](\text{ClO}_4)_2 \cdot 6\text{DMSO}$ (pale red, $0.75 \times 0.60 \times 0.45 \text{ mm}^3$) crystals were collected by means of a conventional Enraf-Nonius CAD4 four-circle diffractometer. Diffraction data for a crystal of succinate-containing complex $2[(3)\text{C}_4\text{H}_4\text{O}_4] \cdot 4\text{DMF}$ (violet, $0.50 \times 0.42 \times 0.33 \text{ mm}^3$; DMF *N,N*-dimethylformamide) were collected by means of a Bruker AXS CCD-based three-circle diffractometer. Both instruments work at ambient temperature with graphite-monochromatized Mo $K\alpha$ X-radiation ($\lambda = 0.71073 \text{ \AA}$). Data reductions for intensities collected with the conventional diffractometer were performed with the *WinGX* package,⁵¹ absorption effects were evaluated with the ψ -scan method,⁵² and absorption correction was applied to the data. Data reduction for frames collected by the CCD-based system were performed with the *SAINT* software;⁵³ absorption effects were empirically evaluated by the *SADABS* software,⁵⁴ and absorption correction was applied to the data. All crystal structures were solved by direct methods (*SIR 97*)⁵⁵ and refined by full-matrix least-squares procedures on F^2 using all reflections (*SHELXL 97*).⁵⁶ Anisotropic displacement parameters were refined for all non-H atoms. H atoms bonded to C atoms were placed at calculated positions with the appropriate AFIX instructions and refined using a riding model; H atoms bonded to secondary amines were located in the final ΔF maps, and their positions were successively refined, restraining the N–H distance to be $0.96 \pm 0.01 \text{ \AA}$.

Crystal data for $[3](\text{ClO}_4)_2$: $\text{C}_{26}\text{H}_{40}\text{Cl}_2\text{CuN}_{12}\text{O}_{14}$, $M = 879.15$, triclinic, $P\bar{1}$ (No. 2), $a = 8.153(4) \text{ \AA}$, $b = 9.129(6) \text{ \AA}$, $c = 13.618(7) \text{ \AA}$, $\alpha = 76.59(5)^\circ$, $\beta = 75.01(5)^\circ$, $\gamma = 68.05(4)^\circ$, $V = 897.7(9) \text{ \AA}^3$, $Z = 1$, 3415 measured reflections, 3162 unique reflections ($R_{\text{int}} = 0.036$), 2321 strong data [$I_0 > 2\sigma(I_0)$], $R1 = 0.0837$ and $wR2 = 0.1185$ for strong data, and $R1 = 0.1743$ and $wR2 = 0.2039$ for all data.

Crystal data for $[3](\text{ClO}_4)_2 \cdot 6\text{DMSO}$: $\text{C}_{38}\text{H}_{76}\text{Cl}_2\text{CuN}_{12}\text{O}_{26}\text{S}_6$, $M = 1347.98$, triclinic, $P\bar{1}$ (No. 2), $a = 10.259(3) \text{ \AA}$, $b = 12.451(3) \text{ \AA}$, $c = 14.554(4) \text{ \AA}$, $\alpha = 66.14(2)^\circ$, $\beta = 74.18(2)^\circ$, $\gamma = 70.85(2)^\circ$, $V =$

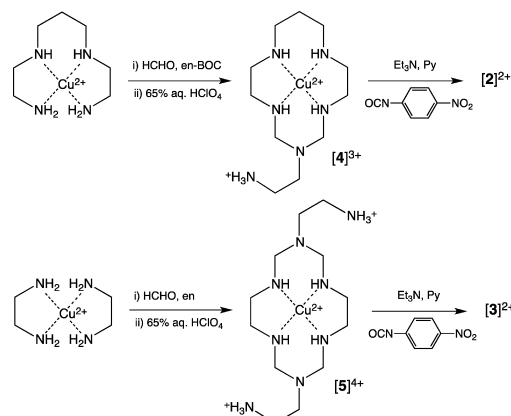
$1584.9(8) \text{ \AA}^3$, $Z = 1$, 7859 measured reflections, 5553 unique reflections ($R_{\text{int}} = 0.021$), 3490 strong data [$I_0 > 2\sigma(I_0)$], $R1 = 0.0641$ and $wR2 = 0.1056$ for strong data, and $R1 = 0.1669$ and $wR2 = 0.1933$ for all data. Positional disorder affects perchlorate counterions and dimethyl sulfoxide solvent molecules [see the Supporting Information (SI) for details].

Crystal data for $2[(3)\text{C}_4\text{H}_4\text{O}_4] \cdot 4\text{DMF}$: $\text{C}_{72}\text{H}_{116}\text{Cu}_2\text{N}_{28}\text{O}_{24}$, $M = 1885.02$, triclinic, $P\bar{1}$ (No. 2), $a = 9.329(1) \text{ \AA}$, $b = 12.550(1) \text{ \AA}$, $c = 18.982(2) \text{ \AA}$, $\alpha = 92.63(1)^\circ$, $\beta = 93.56(1)^\circ$, $\gamma = 101.92(1)^\circ$, $V = 2166.2(4) \text{ \AA}^3$, $Z = 1$, 15742 measured reflections, 7592 unique reflections ($R_{\text{int}} = 0.016$), 6306 strong data [$I_0 > 2\sigma(I_0)$], $R1 = 0.0380$ and $wR2 = 0.0464$ for strong data, and $R1 = 0.1046$ and $wR2 = 0.1117$ for all data.

RESULTS AND DISCUSSION

Synthesis and Crystal Structure of the Macrocyclic Complexes. The copper complexes $[2]^{2+}$ and $[3]^{2+}$ were prepared by a two-step procedure (see Scheme 1) involving (i)

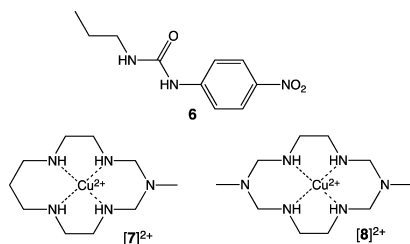
Scheme 1. Synthesis of Complexes $[2]^{2+}$ and $[3]^{2+}$



the metal-templated synthesis of the macrocyclic framework, affording the protonated mono- and diamino intermediates, $[4]^{3+}$ and $[5]^{4+}$, respectively, and (ii) the reaction with (4-nitrophenyl)isocyanate to convert primary amino groups into ureas. Azacyclam complex $[4]^{3+}$ was obtained by a template reaction in which the copper(II) complex of an open tetraamine (2.3.2-tet) is converted into a macrocyclic compound in the presence of formaldehyde and monoprotected ethylenediamine, which behaves as a “locking fragment”.

The diazacyclam complex $[5]^{4+}$ was also prepared according to a template method⁴⁷ in which ethylenediamine acts both as the starting ligand for copper(II) and as the locking fragment. Both intermediates $[4]^{3+}$ and $[5]^{4+}$ were isolated, after the addition of excess perchloric acid, as tri- and tetraperchlorate salts, respectively, with the primary amino groups protonated. The addition of acid induces at the same time deprotection of the primary amino group of the mono-pendant-arm azacyclam derivative. The reaction with (4-nitrophenyl)isocyanate was carried out in anhydrous MeCN in the presence of pyridine.^{57,58}

The mono- and bisurea derivatives $[2]^{2+}$ and $[3]^{2+}$ were satisfactorily characterized by elemental analyses and by FT-IR and ESI-MS. The electronic spectra of complexes $[2]^{2+}$ – $[5]^{4+}$ as well as of the reference urea derivative **6** were measured in MeCN. Solutions with different concentrations (about 10^{-5} and 10^{-3} M) of macrocycle/urea conjugates were examined to accurately detect both the intense bands in the UV range and



the weak bands in the visible range. Absorption data of all of the mentioned compounds and of the reference macrocyclic copper complexes of methylazacyclam, **[7]²⁺**, and dimethyldiazacyclam, **[8]²⁺**, are reported in Table 1.

Table 1. UV–Vis Spectral Data for Copper(II) Aza- and Diazacyclam Complexes and Related Reference Compounds in MeCN

compound	λ (nm)	ϵ (M ⁻¹ cm ⁻¹)
[2]²⁺	335	17050
	501	68
[3]²⁺	336	32800
	498	69
[4]³⁺	500	67
	510 ^a	76 ^a
[5]⁴⁺	496	68
6	336	16500
[7]²⁺	505	75 ^{a,b}
[8]²⁺	498	76 ^{a,c}

^aIn water. ^bReference 60. ^cReference 61.

The strong absorption in the UV region (335–336 nm) can be ascribed to a charge-transfer (CT) transition due to the (nitrophenyl)urea moieties on the pendant arms of compounds **[2]²⁺** and **[3]²⁺**.^{15,44} This band displays a similar intensity in the spectra of complex **[2]²⁺** and of metal-free urea derivative **6**, while it is about 2-fold more intense in the spectrum of **[3]²⁺**, in accordance with the presence of two (nitrophenyl)urea chromophores appended on the macrocyclic complex.

The weak bands observed in the visible region (around 500 nm) must be considered an envelope of the three possible d–d transitions ($xz, yz \rightarrow x^2 - y^2$; $z^2 \rightarrow x^2 - y^2$; $xy \rightarrow x^2 - y^2$) in the copper(II) tetramine chromophore with square-planar coordination geometry.^{44,59} The d–d absorptions in the spectra of **[2]²⁺** and **[3]²⁺** are comparable to those previously reported for plain copper(II) azacyclam, **[7]²⁺**, and diazacyclam, **[8]²⁺**, complexes^{60,61} and to those exhibited by the mono- and bis(ethylammonium) derivatives **[4]³⁺** and **[5]⁴⁺**.

Red crystals of complex salt **[3](ClO₄)₂** suitable for X-ray diffraction studies were obtained by slow diffusion of diethyl ether in an MeCN solution. In a separate experiment, slow diffusion of ethyl acetate in a DMSO solution provided pale-red crystals of **[3](ClO₄)₂·6DMSO**, whose structure has been discussed in the SI (see Figures S1 and S2 and Table S1).

The molecular structure of the copper(II) diazacyclam complex **[3]²⁺** determined on a single crystal of its perchlorate salt is shown in Figure 1.

The molecular structure exhibits *C_i* symmetry with the metal center placed on a crystallographic center of inversion; the macrocyclic diazacyclam ligand adopts the *trans*-III(*R,R,S,S*) configuration⁶² commonly observed in copper(II) cyclam metal complexes. The Cu^{II} center shows a square-planar coordination and lies on the plane defined by the four secondary amines. The

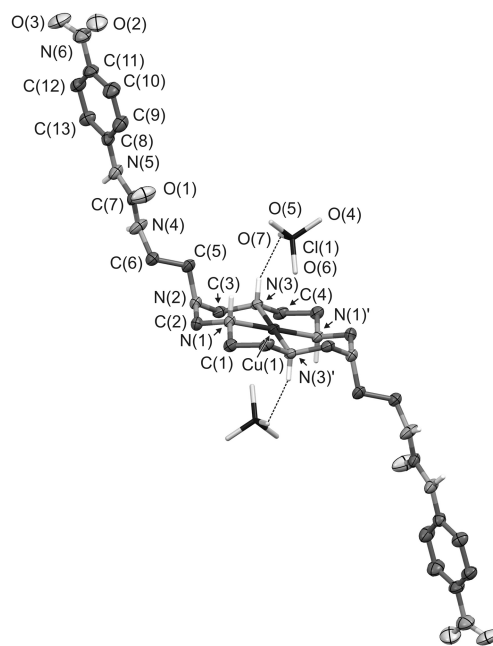


Figure 1. ORTEP view (30% probability level) of the copper(II) diazacyclam complex salt **[3](ClO₄)₂**. Selected bond lengths (Å) and angles (deg): Cu(1)–N(1) 2.009(6), Cu(1)–N(3) 1.999(5), N(1)–Cu(1)–N(3) 94.0(2), N(1)–Cu(1)–N(3)′ 86.0(2). Symmetry code ' = $-x, 1 - y, 1 - z$. Dashed lines indicate hydrogen bonds.

mean Cu^{II}–N distance is 2.00(1) Å, slightly shorter than the value of 2.03 Å reported for the strain-free Cu–N distance.⁶³

The two axial positions corresponding to a rather elongated octahedral coordination for the metal center are occupied by two symmetrically equivalent O(6) atoms of two perchlorate counterions. The observed Cu(1)–O(6) distance of 2.71(1) Å suggests that only a very weak coordinative interaction occurs. In particular, each perchlorate counterion profits from this weak interaction and from an additional hydrogen-bond interaction provided by the N(3) secondary amine, which acts as a H-atom donor. Features of the N–H⋯O interaction are N(3)⋯O(7) 3.11(1) Å, H(3N)⋯O(7) 2.27(5) Å, and N(3)–H(3N)⋯O(7) 146(4)°.

The tertiary amines show a trigonal-pyramidal geometry with N(2) located at only 0.26(1) Å from the basal plane defined by the three C atoms bonded with N. This suggests a pronounced sp² character for the N(2) atom, which is also excluded by any coordinative interaction with the metal center, due to the Cu(1)–N(2) distance of 3.31(1) Å.

The (nitrophenyl)urea pendant arms are almost coplanar, with dihedral angles of 9.7(8)° between the urea group and phenyl ring and 10.3(19)° between the phenyl ring and terminal nitro group. The dihedral angle between the urea and nitro groups is 19.2(15)°.

The NH groups of the urea moieties act as H-atom-donor groups of weak N–H⋯O interactions (*D*⋯*A* > 3.2 Å) involving the O atoms of perchlorate counterions as H-atom-acceptor species. A complete description of hydrogen-bond interactions in the solid state is reported in the SI.

Interaction of **[2]²⁺ with Oxo Anions. Spectrophotometric Studies.** The behavior of anion receptors containing binding groups inclined to form hydrogen bonds, such as urea and thiourea, is usually investigated in aprotic media in order to prevent solvent competition. The present study was performed

in MeCN, in which system $[2]^{2+}$ (as well as $[3]^{2+}$) displays a reasonable solubility.

In particular, the interaction of the copper complex/urea conjugate with anionic species was investigated by spectrophotometric titration experiments in which solutions of tetrabutylammonium salts of the selected anions (usually about 2×10^{-3} M) were added to a solution of $[2]^{2+}$ (about 5×10^{-5} M).

The urea–anion interaction was monitored by observing the changes in the absorption band corresponding to the CT transition (335 nm). This transition generates a partial negative charge on the nitro substituent and a partial positive charge on the NH group belonging to the urea moiety. Therefore, the interaction of a negatively charged species with the urea subunit is expected to stabilize the excited state and, as a consequence, to reduce the transition energy. Thus, the anion–urea interaction should result in a red shift of the absorption band: the stronger the interaction, the larger the resulting $\Delta\lambda$. Nonlinear least-squares treatment of the spectrophotometric titration data allowed evaluation of the stability constants for complex/anion adducts. The corresponding log K values are reported in Table 2.

Table 2. Stability Constants (log K), Determined from UV–Vis Spectral Data, for the Interaction of Anions with Copper(II) Aza- and Diazacyclam Complexes $[2]^{2+}$ and $[3]^{2+}$ and Urea Reference Compound 6 in MeCN

anion	$[2]^{2+}$	$[3]^{2+}$	6
CH_3COO^-	6.03 ± 0.04	$\log K_1 = 6.47 \pm 0.09, \log K_2 = 5.24 \pm 0.09$	4.48 ± 0.03
$\text{C}_6\text{H}_5\text{COO}^-$	5.14 ± 0.01	$\log K_1 = 5.25 \pm 0.04, \log K_2 = 4.71 \pm 0.01$	4.10 ± 0.01
H_2PO_4^-	<i>a</i>	<i>a</i>	3.92 ± 0.01
$\text{HP}_2\text{O}_7^{3-}$	5.36 ± 0.02	7.43 ± 0.06	4.27 ± 0.01
NO_3^-	<2	<2	<2
HSO_4^-	<2	<2	<2

^aPrecipitation occurred during the titration experiment.

At first, a common Y-shaped oxo anion such as acetate was considered because of its well-known tendency to interact with urea derivatives. Spectra taken during the titration of a solution of $[2](\text{ClO}_4)_2$ with a standard solution of tetrabutylammonium acetate are reported in Figure 2.

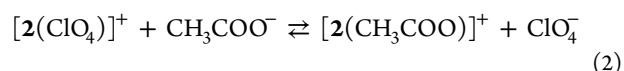
Upon the addition of CH_3COO^- , the band at 335 nm progressively shifts to higher wavelengths up to 353 nm with an

increase of the molar absorbance from 17050 to $19600 \text{ M}^{-1} \text{ cm}^{-1}$. The titration profile obtained by plotting the absorption intensity at 370 nm versus the equivalent ratio (see Figure 2b) indicates a 1:1 stoichiometry for the receptor–acetate interaction. The log K value determined for the equilibrium



is 6.03 ± 0.04 .

It should be noted that a monourea pendant-arm receptor, $[2]^{2+}$, was isolated as perchlorate salt and, as a consequence, ClO_4^- anions are present in solution when spectrophotometric titration is performed. Therefore, the receptor–anion association constant determined by the above-described experiment should be related, in principle, to an “exchange” equilibrium:



However, because of the extremely poor basic and coordinating properties of perchlorate, competition with this anion should be considered negligible.

These data show that the interaction between complex $[2]^{2+}$ and acetate involves the urea pendant arm, as evidenced by the red shift of the (nitrophenyl)urea CT absorption band. Because the low intensity of the d–d band at low concentration levels prevents a clear observation of possible changes, no information about a cooperative effect of the proximate metal center in the anion binding process can be provided by this experiment. Therefore, the titration was repeated on a more concentrated solution of the azacyclam complex $[2]^{2+}$ in MeCN.

Figure 3 shows d–d spectra taken during the titration of a 10^{-3} M solution of $[2]^{2+}$ with $[\text{Bu}_4\text{N}]\text{CH}_3\text{COO}$. The band centered at 501 nm undergoes a shift to higher wavelength ($\lambda = 544 \text{ nm}$) and an intensity increase (up to $102 \text{ M}^{-1} \text{ cm}^{-1}$), until 1 equiv of acetate is added. This behavior suggests that the interaction between the anion and metal center also takes place, inducing a change in the coordination geometry and, as a consequence, in the d–d absorption band. In particular, a change from the square-planar geometry to five-coordination, probably with a square-pyramidal geometry, is caused by the first 1 equiv of added acetate. In fact, the approach of a fifth donor atom along the z axis is expected to raise the energy of the d orbitals with a z component, with a consequent decrease in the energy of the d–d transition envelope, and to cause a red shift of the corresponding band. Moreover, the interaction of an

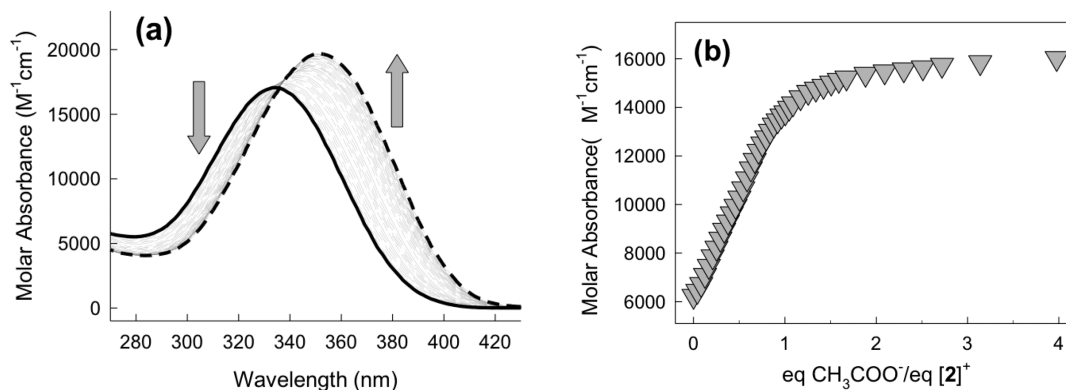


Figure 2. (a) Family of spectra taken in the course of the titration of a 5.4×10^{-5} M solution in $[2](\text{ClO}_4)_2$ with a 2.2×10^{-3} M solution of $[\text{Bu}_4\text{N}]\text{CH}_3\text{COO}$ at 25°C (solid bold line, 0 equiv; dashed bold line, 4 equiv of added acetate). (b) Titration profile at 370 nm indicating the formation of a 1:1 adduct.

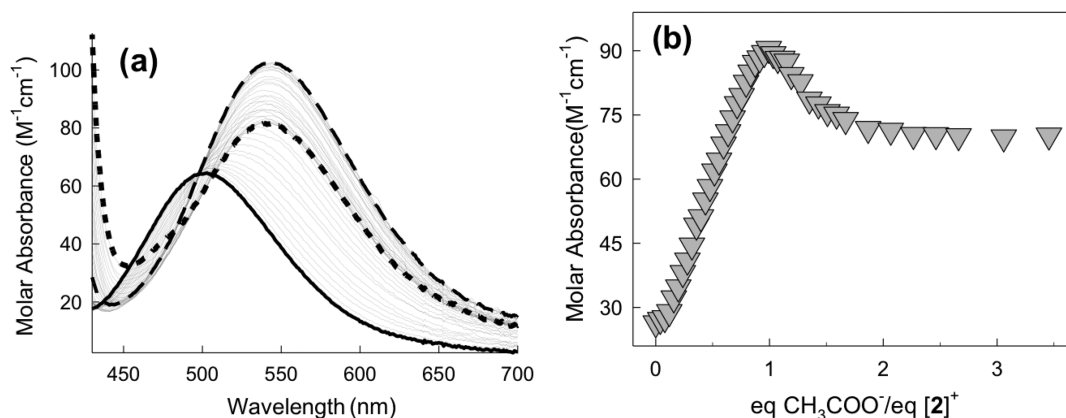


Figure 3. (a) Spectra taken over the course of the titration of a 1.01×10^{-3} M solution of the copper(II) azacyclam complex $[2]^{2+}$ in MeCN with a 2.02×10^{-2} M solution of $[\text{Bu}_4\text{N}]\text{CH}_3\text{COO}$ in MeCN (solid bold line, 0 equiv; dashed bold line, 1 equiv; short-dashed bold line, 3.5 equiv of added acetate). (b) Titration profile at 570 nm.

“axial” ligand induces the loss of the center of symmetry in the azacyclam complex, a circumstance that makes d–d transitions “less” forbidden and increases the absorbance.^{44,64}

The titration profile clearly shows that the band intensity increases until 1 equiv of acetate has been added and then moderately decreases upon the addition of a second 1 equiv ($82 \text{ M}^{-1} \text{ cm}^{-1}$ at 544 nm). This result could be explained by the interaction of a further anion with the metal center, causing a coordination change from a square-pyramidal to an elongated octahedral geometry. The partial symmetry recovery results in a moderate intensity decrease of the d–d absorption. It should be noted that the second 1 equiv of anion interacts only with the metallomacrocyclic subunit of receptor $[2]^{2+}$ because no detectable variations of the band corresponding to the urea subunit were observed after the addition of the first 1 equiv of $[\text{Bu}_4\text{N}]\text{CH}_3\text{COO}$.

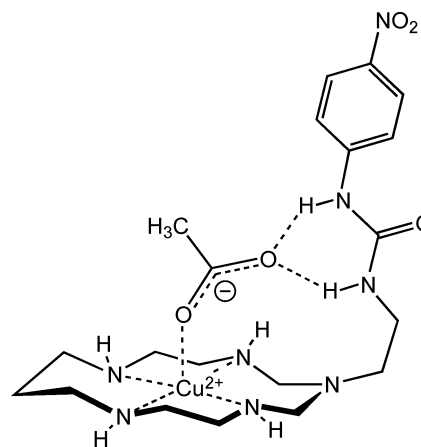
Therefore, UV–vis titration experiments performed at different concentrations indicate that acetate interacts at the same time with both the urea and the metallomacrocyclic subunits of the receptor $[2]^{2+}$. The presence of a metal ion close to the urea groups may favor the binding process not only for electrostatic reasons but also because of the active part played in the recognition process, by establishing coordinative interactions with the anionic substrate.

An analogous investigation was performed on the urea model compound **6** in order to assess the anion binding properties of the (4-nitrophenyl)urea subunit in the absence of any possible cooperative effect due to presence of the metal center. Figure S4 in the SI reports the spectra taken during the titration of a solution of **6** with a standard solution of $[\text{Bu}_4\text{N}]\text{CH}_3\text{COO}$ and the corresponding titration profiles.

The reference system also interacts with acetate, as shown by the red shift of the CT band (from 336 to 364 nm) observed during the addition of the anion solution. The isosbestic point observed along the titration experiment at 344 nm suggests that only two species are present at the equilibrium (**6** and $[\text{6} \cdot \text{CH}_3\text{COO}]^-$). The best fit of the spectrophotometric titration data with a nonlinear least-squares procedure⁴⁸ over the interval 290–390 nm was obtained by assuming a 1:1 equilibrium with a $\log K = 4.48 \pm 0.03$. A comparison of the stability constant values determined for $[\text{6} \cdot \text{CH}_3\text{COO}]^-$ and $[\text{2}(\text{CH}_3\text{COO})]^+$ adducts clearly indicates that the proximity of the Cu^{2+} /macrocycle subunit connected to the urea group distinctly increases its binding properties toward acetate.

Spectral data suggest that the carboxylate group interacts at the same time with both the metal ion and urea pendant arm and a scorpionate-like^{43a,65,66} structure could be assumed for the $[\text{2}(\text{CH}_3\text{COO})]^+$ complex, as sketched in Scheme 2.

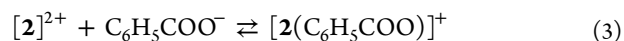
Scheme 2. Sketch of a Hypothesized Structure of the $[\text{2}(\text{CH}_3\text{COO})]^+$ Complex



It should be noted that the carboxylate group interacts with the monourea pendant-arm receptor $[2]^{2+}$ according to a “bridged” mode, while it is expected to behave as a “Y-shaped” anion in the interaction with plain urea. However, the existence of a dynamic equilibrium between different species containing acetate interacting via bridged and Y-fashioned modes cannot be ruled out in solution.

Analogous investigations were carried out with a variety of oxo anions ($\text{C}_6\text{H}_5\text{COO}^-$, NO_3^- , HSO_4^- , H_2PO_4^- , and $\text{HP}_2\text{O}_7^{3-}$).

The addition of tetrabutylammonium benzoate to a MeCN solution of $[2]^{2+}$ induced spectral changes very similar to those observed during the titration experiment with acetate. In particular, the maximum of the band at 335 nm underwent a red shift of 15 nm, and an isosbestic point at 336 nm was observed (Figure S5 in the SI). The $\log K$ value (5.14 ± 0.01) determined for the equilibrium



by nonlinear least-squares treatment of the spectral data is slightly lower than that obtained from titration with acetate (see

Table 2). It can be ascribed to the lower basicity of benzoate and its consequent lower tendency to accept hydrogen bonds if compared with acetate.^{15,29} The adduct formed by benzoate with receptor $[2]^{2+}$ is considerably more stable than the adduct formed with model compound **6** ($\log K = 4.10 \pm 0.01$), as already observed in the case of acetate. This confirms that the proximity of a metal center to the urea subunit increases the stability of the receptor/anion adduct.

Less basic (and, therefore, poorly coordinating) anions such as nitrate and hydrogen sulfate affected to a lower extent the spectral properties of receptor $[2]^{2+}$ than carboxylate anions. As an example, Figure S6 in the SI displays the spectra obtained upon titration with hydrogen sulfate. The band at 335 nm underwent a very small red shift along the titrations with $[\text{Bu}_4\text{N}]\text{NO}_3$ and $[\text{Bu}_4\text{N}]\text{HSO}_4$ (by 4 and 7 nm, respectively) suggesting that only a weak interaction of anionic substrates with the (4-nitrophenyl)urea subunit takes place (receptor–anion association constants lower than 2 log units). Moreover, the d–d band at 501 nm, monitored during analogous titration experiments on more concentrated solutions of the receptor, did not show any significant red shift. The small intensity increase may be ascribed to a precipitation process, as suggested by the baseline increase (Figure S6b in the SI).

Titration with dihydrogen phosphate induced considerable changes in the absorption spectrum of the monourea derivative $[2]^{2+}$. In particular, the band at 335 nm underwent a red shift (to 348 nm) and a progressive intensity decrease, while a simultaneous increase of the baseline was observed (signaling incipient precipitation), which prevented completion of the titration experiment (Figure S7 in the SI). The shift of the CT band to higher wavelength suggests that an interaction of the anion with the (nitrophenyl)urea subunit takes place, as already observed in the case of acetate and benzoate. On the other hand, an absorption intensity decrease and a spectrum baseline increase are usually consistent with the formation of a poorly soluble species during the titration (for instance, the 1:2 neutral complex). The precipitation lowers the complex concentration and absorption intensity and generates turbidity of the solution and a shift of the spectrum baseline. Therefore, the spectral data obtained by this titration experiment did not allow an accurate determination of the adduct stoichiometry and of the corresponding stability constant value. Any attempt to perform a similar experiment at a lower concentration did not provide better results.

In order to have better insight into the affinity of $[2]^{2+}$ toward anions of the phosphate family, the receptor's behavior in solution was also investigated in the presence of pyrophosphate. It should be noted that di- and polyphosphate anions, which participate in several bioenergetic and metabolic processes,^{5,67} represent relevant targets in anion recognition and sensing. Spectra collected during the titration experiment with $[\text{Bu}_4\text{N}]_3\text{HP}_2\text{O}_7$ and the corresponding titration profile are reported in Figure S8 in the SI. In this case also, the band at 335 nm was shifted to higher wavelengths ($\lambda_{\text{max}} = 360$ nm) and its intensity increased ($\epsilon_{\text{max}} = 19700$), suggesting a strong interaction of the oxo anion with the urea moiety. The molar absorbance versus equivalent ratio plot clearly indicates that the monourea pendant-arm complex $[2]^{2+}$ interacts with pyrophosphate according to a 1:1 stoichiometry even if no isosbestic point is observed in the absorption spectra during the titration experiment. The presence of more than one complex species in solution can be explained with the structural features of the dimeric phosphate anion, which could interact in an

intermolecular fashion with two binding sites (namely, urea and metal center) located on different receptor molecules at the same time. Therefore, the formation of receptor/anion adducts with different stoichiometric ratios (e.g., 2:1 or 3:2) could be expected at low concentrations of anion (receptor/anion molar ratio >1), as also suggested by the titration profile displaying an inflection point at an anion/receptor molar ratio of close to 0.5. The best fit of the titration data was obtained by assuming the formation of 1:1 species, and the $\log K$ value for the $[2(\text{HP}_2\text{O}_7)]^-$ adduct was 5.36 ± 0.02 .

An analogous titration experiment performed on the urea model compound **6** showed that pyrophosphate interacts with (nitrophenyl)urea according to 1:1 stoichiometry (see Figure S9 in the SI) with $\log K = 4.27 \pm 0.01$. The $[\text{6-HP}_2\text{O}_7]^{3-}$ adduct is distinctly less stable than the 1:1 complex formed by $[2]^{2+}$ with pyrophosphate, confirming again the relevant contribution of the proximal metal center to the anion recognition process.

Titration with $[\text{Bu}_4\text{N}]_3\text{HP}_2\text{O}_7$ was performed also on a more concentrated MeCN solution of $[2]^{2+}$ in order to monitor the changes experienced by the d–d band and to assess the interaction of pyrophosphate with the metal center. The band centered at 501 nm underwent a red shift ($\Delta\lambda = 35$ nm) and an intensity increase in the course of the titration ($\epsilon_{\text{max}} = 106 \text{ M}^{-1} \text{ cm}^{-1}$ at 536 nm after the addition of 1 equiv of anion), as shown in Figure S10a in the SI. The titration profile suggests that an interaction according to an 1:1 stoichiometry takes place, although a precipitation process, which occurred in the presence of excess anion, did not allow determination of the corresponding equilibrium constant (see Figure S10b in the SI). Variations of the d–d band are consistent with a change of the copper(II) coordination geometry from square-planar to square-pyramidal and clearly indicate that the metal ion is directly involved in the recognition process.

Changes of both the CT and d–d bands observed during the titration experiments suggest that one anion interacts at the same time with the (nitrophenyl)urea group and metal-lomacrocyclic subunit. Therefore, it may be assumed that pyrophosphate is bound according to a “bridged mode”, providing a scorpionate-like structure. Unfortunately, although there have been several attempts to isolate the adduct in crystalline form, no crystals suitable for X-ray crystallographic studies were obtained and the hypothesis of the scorpionate-type adducts formed by the monourea derivative $[2]^{2+}$ cannot be supported by structural data directly concerning this complex.

Titration experiments with selected oxo anions (CH_3COO^- , HSO_4^- , H_2PO_4^- , and $\text{HP}_2\text{O}_7^{3-}$) were also performed on reference macrocyclic complex $[7]^{2+}$,⁶⁰ in order to estimate the contribution of the coordinative interaction involving the metalloazacyclam subunit on the stability of the receptor $[2]^{2+}$ /anion adduct. It should be noted that these experiments were carried out on solutions of ca. 10^{-3} M of the complex to allow monitoring of the low-intensity d–d band. Unfortunately, the addition of any of the considered anions induced precipitation, preventing determination of the constant values associated with the formation of adducts. As an example, spectra collected during titration of the copper(II) azacyclam complex $[7]^{2+}$ with $\text{HP}_2\text{O}_7^{3-}$ are reported in Figure S11 in the SI.

Interaction of $[3]^{2+}$ with Oxo Anions. Titration experiments in MeCN analogous to those described in the previous section were also performed to investigate the solution behavior

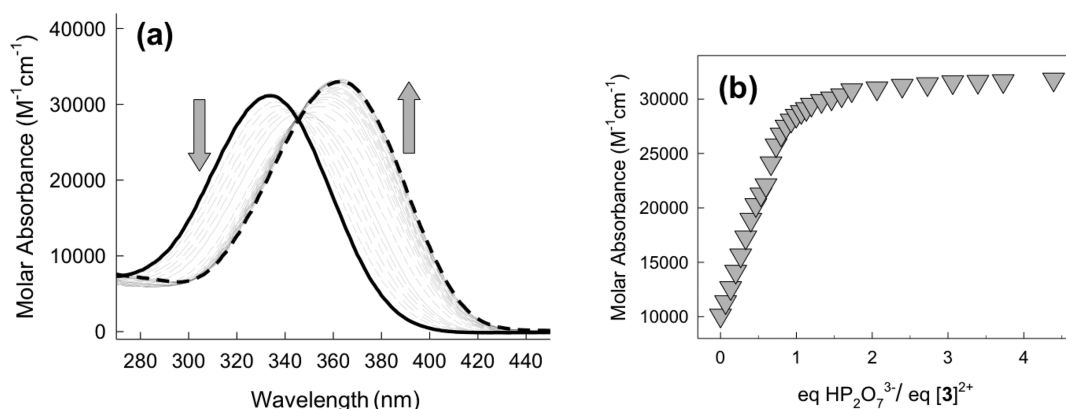


Figure 4. (a) Family of spectra taken in the course of the titration of a 2.5×10^{-5} M solution of $[3](\text{ClO}_4)_2$ in MeCN with a standard solution (2.1×10^{-3} M) of $[\text{Bu}_4\text{N}]_3\text{HP}_2\text{O}_7$ at 25°C (solid bold line, 0 equiv; dashed bold line, 5.2 equiv of added anion). (b) Titration profile at 370 nm.

of bisurea pendant-arm complex $[3]^{2+}$ in the presence of different oxo anions.

The addition of acetate considerably affected the absorption spectrum of the complex: the strong absorption band at 336 nm undergoes a red shift ($\Delta\lambda = 25$ nm) and an intensity increase (ϵ from 32800 to 38900 $\text{M}^{-1}\text{cm}^{-1}$) in the course of the titration (see Figure S12a in the SI). The spectral changes are observed until 2 equiv of anion was added to the complex solution. The 1:2 (receptor/anion) stoichiometry of the final adduct was confirmed by the titration profiles reported in the SI. Moreover, the best fit of the titration data was obtained by assuming the formation of 1:1 and 1:2 complex species according to two stepwise processes:



The log K values determined for these equilibria are 6.47 ± 0.09 and 5.24 ± 0.09 , respectively.

The interaction with acetate also modifies the d–d absorption band, as shown by the titration experiment performed on a more concentrated (10^{-3} M) solution of $[3]^{2+}$. The band at 498 nm undergoes a red shift and an intensity increase, as already observed for the monoureafunctionalized complex (see Figure S13 in the SI). Unfortunately, precipitation occurs even during the addition of the first 1 equiv of anion, preventing completion of the titration experiment.

The behavior of $[3]^{2+}$ in the presence of benzoate is quite similar to that found for acetate. Spectral changes observed during the titration experiments indicate that the overall receptor–anion interaction can be described also in this case by a stepwise process analogous to that described by eqs 4 and 5, but the corresponding association constants are smaller (log $K_1 = 5.25 \pm 0.04$; log $K_2 = 4.71 \pm 0.01$) if compared to those obtained for acetate, as expected on the basis of the lower intrinsic basicity of benzoate.^{15,29}

The spectrophotometric titration experiments performed with acetate and benzoate indicate that the bisurea pendant-arm complex $[3]^{2+}$ interacts in solution with 1 or 2 equiv of carboxylate, depending on its concentration. Each carboxylate group establishes both hydrogen bonds with urea groups on the pendant arms and coordinative interactions at the apical positions of the metal center. These simultaneous interactions should induce the folding of the pendant arm(s), generating

scorpionate-like structures analogous to the one proposed for $[2(\text{CH}_3\text{COO})]^+$ and sketched in Scheme 2. In particular, mono- or discorpionate structures could be expected for 1:1 and 1:2 adducts, respectively.

The poorly coordinating and nonbasic anions NO_3^- and HSO_4^- did not significantly affect the CT and d–d absorption bands of receptor $[3]^{2+}$, confirming their low tendency to interact with both the (nitrophenyl)urea moiety and copper(II) macrocyclic complex subunit, as already observed for the mono-pendant-arm analogue $[2]^{2+}$.

The addition of dihydrogen phosphate induced a progressive precipitation with a consequent absorbance decrease and baseline increase; therefore, the titration experiment could not be completed (see Figure S14 in the SI). However, a change of the CT band could be observed before complete precipitation, indicating that hydrogen-bond interaction with urea subunits takes place. The poor quality of the spectral data did not allow assessment of the stoichiometry of the receptor/anion adduct or the accurate determination of the corresponding association constant(s).

Different from H_2PO_4^- , pyrophosphate did not induce precipitation at low concentration levels of the complex ($<10^{-4}$ M) and titration experiments were successfully performed in order to monitor the CT band. The distinct red shift of the band at 336 nm ($\Delta\lambda = 27$ nm) again supports hydrogen-bond interactions involving the (nitrophenyl)urea pendant arms (Figure 4). The changes of the d–d band at 498 nm could not be completely monitored because of a progressive precipitation during the titration experiment performed on a more concentrated solution of $[3]^{2+}$. Nevertheless, the variations observed after the first additions of anion (intensity increase and shift to higher wavelength) indicate that the coordinative environment of copper(II) undergoes a drastic change due to pyrophosphate coordination.

Quite surprisingly, the titration profiles determined at different wavelength values seem to indicate that a 1:1 adduct is formed in solution. In addition, the best fit of the spectral data was obtained when the formation of only the 1:1 adduct was assumed. The corresponding log K value was 7.43 ± 0.06 . This behavior can be explained by assuming that the formation of the 1:2 species might be prevented by an electrostatic repulsion due to the high negative charge (3^-) on each pyrophosphate anion.

The copper(II) diazacyclam complex $[8]^{2+}$,⁶¹ which can be considered as a reference compound for the study of receptor

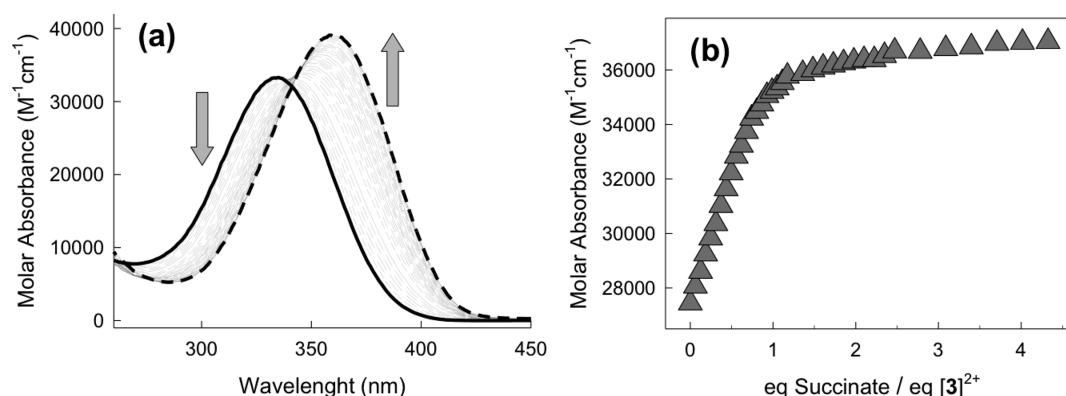


Figure 5. (a) Spectra taken over the course of the titration of a MeCN solution of $[3](\text{ClO}_4)_2$ (2.5×10^{-5} M) with a standard solution (2.0×10^{-3} M) of $[\text{Bu}_4\text{N}]_2(\text{succinate})$ at 25 °C (solid bold line, 0 equiv; dashed bold line, 4.4 equiv of added anion). (b) Titration profile at 350 nm.

$[3]^{2+}$ –anion interaction, was also investigated by titration experiments with oxo anions. As already observed for the azacyclam analogue $[7]^{2+}$ (see above), insoluble material formed upon the addition of anions and spectral data could not be used to calculate the stability constants of the adducts. As an example, spectra registered during the titration of $[8]^{2+}$ with acetate are reported in Figure S15 in the SI.

Interaction of $[3]^{2+}$ with Dicarboxylates. Spectrophotometric titration experiments performed on $[2]^{2+}$ and $[3]^{2+}$ clearly indicate that carboxylate and phosphate anions interact with both complexes by establishing at the same time a coordinative bond with the metal ion and hydrogen bonds with the urea subunit(s) on the pendant arm(s). On the basis of the spectrophotometric studies in solution, we can assume that carboxylate as well as phosphate groups behave as ditopic species and interact according to a bridging mode, as sketched in Scheme 2. However, other interaction modes cannot be ruled out, particularly in the case of the bisurea derivative $[3]^{2+}$, and, in principle, several equilibria involving different species could take place in solution.

In order to investigate the behavior of $[3]^{2+}$ in the presence of genuine ditopic anionic species, titration experiments with selected dicarboxylate compounds were performed. In particular, spectrophotometric titrations were carried out with malonate, $\text{CH}_2(\text{COO}^-)_2$, succinate, $(\text{CH}_2)_2(\text{COO}^-)_2$, and glutarate, $(\text{CH}_2)_3(\text{COO}^-)_2$. The addition of dicarboxylate to the solution of the bisurea pendant-arm macrocyclic complex induces a progressive shift of the band at 335 nm to higher wavelengths, as already observed in the titration experiment with acetate. Similar families of spectra were obtained for the three anionic species, with large $\Delta\lambda$ values (24, 25, and 24 nm for malonate, succinate, and glutarate, respectively) and moderate intensity increase. Figure 5a reports the spectra taken during the titration with succinate, while Figures S16 and S17 in the SI display the families of spectra obtained upon titration with malonate and glutarate, respectively.

Plots of molar absorbance versus equivalent ratio at significant wavelengths indicate that the interaction of $[3]^{2+}$ with all of the considered dicarboxylates occurs according to a 1:1 stoichiometry. In Figure 5b, the plot obtained for succinate at 350 nm is reported as an example.

Although the titration experiments suggest that 1:1 adducts are formed in solution, nonlinear least-squares treatment of the spectral data do not allow calculation of accurate values of association constants. This should be due to the rather large number of equilibria that can take place in solution because

different interaction modes involving at the same time two carboxylate groups (from the anion side) and three binding sites (metal center and two urea subunits from the receptor side) can be hypothesized. Titration experiments performed at higher concentration (1.0×10^{-3} M) in order to monitor the d–d band variations induced by dicarboxylate addition could not be completed because precipitation occurred in all cases before the first 1 equiv of anion was added. However, the red shift and intensity increase of the band centered at 498 nm, which were observed before precipitation occurred, suggest again that the metal center directly contributes to the interaction with the anionic species by establishing axial coordinative bond(s) (see Figure S18 in the SI).

More information about the structure of dicarboxylate/ $[3]^{2+}$ adducts was provided by crystallographic studies. In fact, upon slow diffusion of diethyl ether into a DMF/MeCN solution (1:1 by volume) containing equimolar amounts of $[\text{Bu}_4\text{N}]_2(\text{succinate})$ and $[3](\text{ClO}_4)_2$, violet crystals of the resulting 1:1 adduct, suitable for X-ray diffraction studies, were obtained.

The crystal contains two symmetrically independent $[\text{Cu}^{\text{II}}(3)]^{2+}$ molecular cations, each interacting with two succinate anions and four additional DMF solvent molecules: $2([\text{3}]\text{C}_4\text{H}_4\text{O}_4) \cdot 4\text{DMF}$ ($\text{C}_4\text{H}_4\text{O}_4 = \text{succinate}$). One of the two very similar but nonsymmetrically equivalent $[\text{Cu}^{\text{II}}(3)]^{2+}$ molecular cations and the interacting oxo anions are shown in Figure 6 (see Figure S19 in the SI for the ORTEP view of the other molecular cation). Both nonsymmetrically equivalent copper(II) diazacyclam subunits exhibit C_2 symmetry: the two Cu^{II} metal centers are placed on two crystallographic centers of inversion, and both copper ions lie in the plane of the four-amine donor set. Both diazacyclam ligands adopt the *trans*-III(*R,R,S,S*) configuration. The mean values for the Cu–N bonds are slightly longer than those observed in the structure of the bisurea diazacyclam complex $[3]^{2+}$ (without oxoanions): the mean value of 2.02(1) Å for both the Cu(1) and Cu(2) centers in the succinate adduct should be compared to the mean value of 2.00(1) Å observed in the structure shown in Figure 1.

Very interestingly, each carboxylate group of the succinate ions interacts with receptor $[3]^{2+}$ according to a “bridged” mode: one O atom of $-\text{COO}^-$ is located on an axial position of the elongated octahedral coordination exhibited by the Cu^{II} center, while the other O atom acts as a H-atom acceptor of three hydrogen bonds, two of which are provided by the two NH groups of urea.

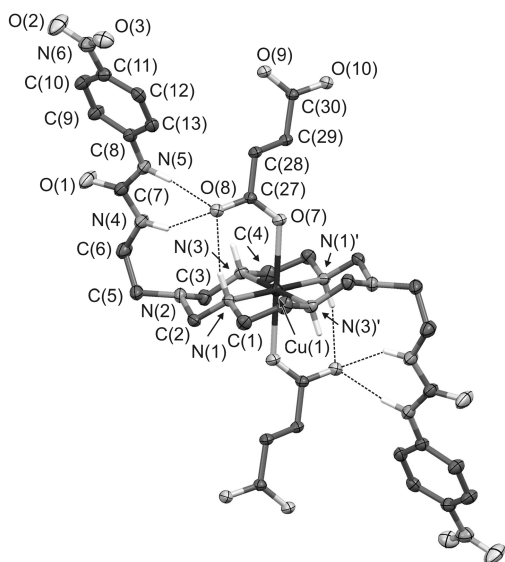


Figure 6. ORTEP view (30% probability level) of one $[3]^{2+}$ molecular cation interacting with succinate oxo anions. Selected bond lengths (Å) and angles (deg): Cu(1)–N(1) 2.008(2), Cu(1)–N(3) 2.032(2), Cu(1)–O(7) 2.425(2); N(1)–Cu(1)–N(3) 93.7(1), N(1)–Cu(1)–N(3)' 86.3(1), N(1)–Cu(1)–O(7) 91.2(1), N(3)–Cu(1)–O(7) 89.8(1). Symmetry code ' : $1 - x, 1 - y, 1 - z$. Dashed lines indicate hydrogen bonds.

The direct interaction of carboxylates with the metal center is very similar for the two nonequivalent Cu^{II} centers: the observed distances are Cu(1)–O(7) 2.43(1) Å and Cu(2)–O(9) 2.44(1) Å.

The “bridged” interaction mode of each carboxylic group is determined by two asymmetric N–H \cdots O bonds provided by the urea group on a pendant arm and by a single N–H \cdots O bond provided by a secondary amine of the macrocycle. The two asymmetric H \cdots O distances for the hydrogen bonds involving urea NH groups are 1.90(2) and 2.16(2) Å and 1.83(2) and 2.29(2) Å for the two independent molecular complexes, respectively, with the shortest H \cdots O distance being provided by the urea NH group close to the terminal nitrophenyl group. The H \cdots O distances of the single N–H \cdots O bond provided by the secondary amine of the macrocycle are 2.13(1) and 2.09(1) Å for the two independent molecular complexes, respectively. These values are intermediate between those observed for the urea NH groups.

Because each succinate ion interacts at the same time with the metal centers of two nonsymmetrically equivalent adjacent molecules, molecular chains extending along the c -axis direction originate in the solid state. A portion of a molecular chain is shown in Figure 6, and the geometrical features of the hydrogen-bond interactions are reported in Table 3.

Crystallographic studies performed on the $[3]^{2+}$ /succinate adduct show that ditopic anions such as aliphatic dicarboxylates preferentially establish “intermolecular” interactions with the investigated macrocyclic systems. However, the structure represented in Figure 7 describes the most stable (or one of the most stable) molecular arrangement in the solid state, and other different structures could be hypothesized in solution.

On the other hand, it is important to point out that the simultaneous interaction of carboxylate species with the Cu^{II} ion and the urea group belonging to the same macrocyclic complex is structurally allowed. In particular, the urea-containing pendant arms can be folded in order to establish

Table 3. Features of Hydrogen Bonds in the $2([3]^{2+})(\text{C}_4\text{H}_4\text{O}_4) \cdot 4\text{DMF}$ Crystal

donor group D	D \cdots A (Å)	H \cdots A (Å)	D–H \cdots A (deg)	acceptor atom A
N(1)–H(1N)	3.01(1)	2.13(1)	156(1)	O(8)
N(4)–H(4N)	3.02(1)	2.16(2)	148(2)	O(8)
N(5)–H(5N)	2.83(1)	1.90(2)	166(2)	O(8)
N(3)–H(3N)	3.17(1)	2.45(2)	133(1)	O(11)
N(9)–H(9N)	2.98(1)	2.09(1)	159(1)	O(10)
N(10)–H(10N)	3.13(1)	2.29(2)	147(2)	O(10)
N(11)–H(11N)	2.77(1)	1.83(2)	173(2)	O(10)
N(7)–H(7N)	2.92(1)	2.13(2)	141(1)	O(12)

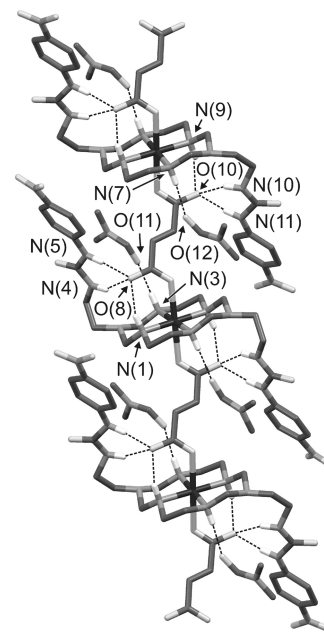


Figure 7. Simplified sketch of the hydrogen bonds in $2([3]\text{C}_4\text{H}_4\text{O}_4) \cdot 4\text{DMF}$ crystal. Atom names identify the independent hydrogen-bond interactions.

the bifurcated hydrogen bonds with the $-\text{COO}^-$ moiety, as shown by the scorpionate-like structure hypothesized in Scheme 2. This conformation can be adopted by complex $[3]^{2+}$, and similarly by $[2]^{2+}$, even in the recognition in solution of simpler anionic species such as acetate and related monocarboxylates.

CONCLUSIONS

This paper has confirmed the role of metal complexes, in particular those with functionalized macrocyclic ligands, as useful platforms in the design of synthetic receptors for anions. Among macrocyclic complexes, aza- and diazacyclam systems can be easily prepared by template syntheses and functionalized with different groups. In particular, the introduction of one or two urea subunits on the macrocyclic framework of the ligands described in this paper provides multicomponent systems that can interact with anionic substrates by both coordinative interactions (metal center) and hydrogen bonds (urea subunits).

The investigated copper(II) complexes $[2]^{2+}$ and $[3]^{2+}$, carrying one and two urea pendant arms, respectively, recognize anionic species displaying a coordinating tendency

toward copper(II) and a good affinity toward urea subunits at the same time, namely, carboxylates and phosphates.

In particular, $[2]^{2+}$ forms 1:1 adducts with acetate, benzoate, hydrogendiphosphate, and dihydrogen phosphate, although in the latter case, an insoluble product is obtained. Stability constants of the adducts are considerably higher than the ones determined for the interaction of the same anions with plain urea reference compound **6**, confirming the synergistic action of metallomacrocyclic and urea subunits. Complex $[3]^{2+}$ interacts with the same anions according to 1:1 and 1:2 stoichiometries, with the exception of hydrogendiphosphate, which forms just the 1:1 adduct with a distinctly high association constant ($\log K > 7$).

Spectrophotometric investigations suggest that oxo-anionic species interact according to a “bridged” mode, inducing the macrocyclic systems to adopt a scorpionate-like conformation, which is confirmed by crystallographic studies performed on the $[3]^{2+}$ /succinate adduct. Although different binding modes, for instance, “intermolecular” ones, cannot be ruled out in solution, it should be considered that “intramolecular” interactions should prevail at low concentration levels.

Other common anions such as chloride, hydrogensulfate, and nitrate interact only to a poorly significant extent with both investigated complexes.

The macrocyclic systems studied in this work are scarcely soluble in water. This represents a drawback because they cannot be used in aqueous solutions where receptors for anions usually find practical applications. Moreover, they do not display a very high selectivity toward a specific substrate but toward two classes of compounds. Nevertheless, the investigation about their behavior with carboxylate and phosphate derivatives can relevantly contribute to the development of novel and more effective systems for anion recognition involving both metal–ligand and hydrogen-bond interactions. In particular, the following interesting features should be considered: (i) owing to their high kinetic resistance to demetalation, aza- and diazacyclam macrocyclic complexes are stable even in particular conditions, for instance, in the presence of a large excess of anions or in strongly acidic media; (ii) solubility in water can be improved by introducing more hydrophilic group on the pendant arms; (iii) macrocyclic complex/urea conjugates could be easily employed to prepare functionalized solid phases.

The incorporation of macrocyclic complex/urea conjugate structures, similar to $[2]^{2+}$ and $[3]^{2+}$, into polymeric materials and embedding them in a solid phase are currently under investigation. The resulting product will be tested to selectively remove selected anionic species from aqueous solutions or to preconcentrate them before chromatographic analyses.

■ ASSOCIATED CONTENT

■ Supporting Information

X-ray crystallographic data in CIF format, comment to the crystal structure of $[3](\text{ClO}_4)_2 \cdot 6\text{DMSO}$, Figures S1–S19, and Tables S1 and S2. This material is available free of charge via the Internet at <http://pubs.acs.org>.

■ AUTHOR INFORMATION

Corresponding Author

*E-mail: maurizio.licchelli@unipv.it

Notes

The authors declare no competing financial interest.

■ ACKNOWLEDGMENTS

Financial support of the Italian Ministry for Education, Universities and Research (MIUR), is gratefully acknowledged (Project PRIN2010 010CX2TLM_009). Thanks are due to Dr. Luca Pasotti for assistance with the NMR measurements.

■ REFERENCES

- (1) *Supramolecular Chemistry of Anions*; Bianchi, A., Bowman-James, K., García-España, E., Eds.; Wiley-VCH: New York, 1997.
- (2) (a) Sessler, J. L.; Gale, P. A.; Cho, W.-S. *Anion Receptor Chemistry*; Royal Society of Chemistry: Cambridge, U.K., 2006. (b) Gale, P. A.; Busschaert, N.; Haynes, C. J. E.; Karagiannidis, L. E.; Kirby, I. L. *Chem. Soc. Rev.* **2014**, 43, 205–241.
- (3) *Anion Coordination Chemistry*; Bowman-James, K., Bianchi, A., García-España, E., Eds.; Wiley-VCH: Weinheim, Germany, 2012.
- (4) (a) Hua, Y.; Flood, A. H. *Chem. Soc. Rev.* **2010**, 39, 1262–1271. (b) O’Neil, E. J.; Smith, B. D. *Coord. Chem. Rev.* **2006**, 250, 3068–3080.
- (5) Kubik, S. In *Anion Coordination Chemistry*; Bowman-James, K., Bianchi, A., García-España, E., Eds.; Wiley-VCH: Weinheim, Germany, 2012; p 363.
- (6) Lehn, J.-M. *Supramolecular Chemistry. Concepts and Perspectives*; Wiley-VCH: Weinheim, Germany, 1995.
- (7) (a) Beer, P. D.; Gale, P. A. *Angew. Chem., Int. Ed.* **2001**, 40, 486–516. (b) Caballero, A.; Zapata, F.; Beer, P. D. *Coord. Chem. Rev.* **2013**, 257, 2434–2455.
- (8) Schmidtchen, F. P.; Berger, M. *Chem. Rev.* **1997**, 97, 1609–1646.
- (9) (a) Casasus, R.; Aznar, E.; Marcos, M. D.; Martínez-Mañez, R.; Sançenón, F.; Soto, J.; Amorós, P. *Angew. Chem., Int. Ed.* **2006**, 45, 6661–6664. (b) Santos-Figueroa, L. E.; Moragues, M. E.; Climent, E.; Agostini, A.; Martínez-Mañez, R.; Sançenón, F. *Chem. Soc. Rev.* **2013**, 42, 3489–3613.
- (10) (a) Gale, P. A., Gunnlaugsson T., Guest Eds. *Chem. Soc. Rev.* **2010**, 3581–4008 (themed issue on: Supramolecular chemistry of anionic species). (b) Gale, P. A.; Caltagirone, C. *Chem. Soc. Rev.* **2014**, DOI: 10.1039/c4cs00179f.
- (11) *Anion Sensing, Topics in Current Chemistry*; Stibor, I., Ed.; Springer: Berlin, 2005.
- (12) (a) Snowden, T. S.; Anslyn, E. V. *Curr. Opin. Chem. Biol.* **1999**, 3, 740–746. (b) Wiskur, S. L.; Ait-Haddou, H.; Lavigne, J. J.; Anslyn, E. V. *Acc. Chem. Res.* **2001**, 34, 963–972. (c) Ghosh, K.; Sarkar, A. R.; Sarkar, T.; Panja, S.; Kar, D. *RSC Adv.* **2014**, 4, 20114–20130.
- (13) Graf, E.; Lehn, J.-M. *J. Am. Chem. Soc.* **1976**, 98, 6403–6405.
- (14) Schmidtchen, F. P. *Angew. Chem., Int. Ed. Engl.* **1977**, 16, 720–721.
- (15) Boiocchi, M.; Del Boca, L.; Esteban Gomez, D.; Fabbri, L.; Licchelli, M.; Monzani, E. *J. Am. Chem. Soc.* **2004**, 126, 16507–16514.
- (16) Bondy, C. R.; Loeb, S. J. *Coord. Chem. Rev.* **2003**, 240, 77–99.
- (17) (a) Choi, K.; Hamilton, A. D. *Coord. Chem. Rev.* **2003**, 240, 101–110. (b) Cigañ, M.; Jakusova, K.; Donovalova, J.; Szöcs, V.; Gaplovsky, A. *RSC Adv.* **2014**, 4, 54072–54079.
- (18) Kang, S. O.; Hossain, M. A.; Bowman-James, K. *Coord. Chem. Rev.* **2006**, 250, 3038–3052.
- (19) Blondeau, P.; Segura, M.; Perez-Fernandez, R.; de Mendoza, J. *Chem. Soc. Rev.* **2007**, 36, 198–210.
- (20) García-España, E.; Díaz, P.; Llinares, J. M.; Bianchi, A. *Coord. Chem. Rev.* **2006**, 250, 2952–2986.
- (21) Bazzicalupi, C.; Bencini, A.; Lippolis, V. *Chem. Soc. Rev.* **2010**, 39, 3709–3728.
- (22) Kang, S. O.; Llinares, J. M.; Day, V. W.; Bowman-James, K. *Chem. Soc. Rev.* **2010**, 39, 3980–4003.
- (23) Mateus, P.; Bernier, N.; Delgado, R. *Coord. Chem. Rev.* **2010**, 254, 1726–1747.
- (24) Smith, P. J.; Reddington, M. V.; Wilcox, C. S. *Tetrahedron Lett.* **1992**, 41, 6085–6088.
- (25) Fan, E.; van Arman, S. A.; Kincaid, S.; Hamilton, A. D. *J. Am. Chem. Soc.* **1993**, 115, 369–370.

- (26) Fitzmaurice, R. J.; Kyne, G. M.; Douheret, D.; Kilburn, J. D. *J. Chem. Soc., Perkin Trans. 1* **2002**, 841–864.
- (27) Gale, P. A. *Coord. Chem. Rev.* **2003**, *240*, 191–221.
- (28) Kubik, S.; Reyheller, C.; Stüwe, S. *J. Inclusion Phenom. Macrocyclic Chem.* **2005**, *52*, 137–187.
- (29) Esteban Gómez, D.; Fabbriizzi, L.; Licchelli, M.; Monzani, E. *Org. Biomol. Chem.* **2005**, 1495–1500.
- (30) Esteban-Gómez, D.; Fabbriizzi, L.; Licchelli, M.; Sacchi, D. *J. Mater. Chem.* **2005**, *15*, 2670–2675.
- (31) Lin, Y.-S.; Tu, G.-M.; Lin, C.-Y.; Chang, Y.-T.; Yen, Y.-P. *New J. Chem.* **2009**, *33*, 860–867.
- (32) Fang, A.-I.; Wang, J.-H.; Wang, F.; Jiang, Y.-B. *Chem. Soc. Rev.* **2010**, *39*, 3729–3745.
- (33) Santos-Figueroa, L. E.; Moragues, M. E.; M. Raposo, M. M.; Batista, R. M. F.; Ferreira, R. C. M.; Costa, S. P. G.; Sancenón, F.; Martínez-Máñez, R.; Soto, J.; Ros-Lis, J. V. *Tetrahedron* **2012**, *68*, 7179–7176.
- (34) (a) Mercer, D. J.; Stephen J. Loeb, S. J. *Chem. Soc. Rev.* **2010**, *39*, 3612–3620. (b) Steed, J. W. *Chem. Soc. Rev.* **2009**, *38*, 506–519. (c) Rice, C. R. *Coord. Chem. Rev.* **2006**, *250*, 3190–3199.
- (35) (a) Amendola, V.; Boiocchi, M.; Colasson, B.; Fabbriizzi, L.; Rodriguez Douton, M.-J.; Ugozzoli, F. *Angew. Chem., Int. Ed.* **2006**, *118*, 7074–7078. (b) Amendola, V.; Boiocchi, M.; Colasson, B.; Fabbriizzi, L. *Inorg. Chem.* **2006**, *45*, 6138–6147. (c) Amendola, V.; Boiocchi, M.; Colasson, B.; Fabbriizzi, L.; Monzani, E.; Douton-Rodriguez, M.-J.; Spadini, C. *Inorg. Chem.* **2008**, *47*, 4808–4816.
- (36) Fabbriizzi, L.; Poggi, A. *Chem. Soc. Rev.* **2013**, *42*, 1681–1699.
- (37) (a) Fabbriizzi, L.; Licchelli, M.; Parodi, L.; Poggi, A.; Taglietti, A. *J. Fluoresc.* **1998**, *8*, 263–271. (b) Fabbriizzi, L.; Faravelli, I.; Francese, G.; Licchelli, M.; Perotti, A.; Taglietti, A. *Chem. Commun.* **1998**, 971–972. (c) Fabbriizzi, L.; Licchelli, M.; Perotti, A.; Poggi, A.; Rabaioli, G.; Sacchi, D.; Taglietti, A. *J. Chem. Soc., Perkin Trans. 2* **2001**, 2108–2113. (d) Bergamaschi, G.; Boiocchi, M.; Perrone, M. L.; Poggi, A.; Viviani, I.; Amendola, V. *Dalton Trans.* **2014**, *43*, 11352–11360.
- (38) (a) Ngo, H. T.; Liu, X.; Jolliffe, K. A. *Chem. Soc. Rev.* **2012**, *41*, 4928–4965. (b) Butler, S. J.; Parker, D. *Chem. Soc. Rev.* **2013**, *42*, 1652–1666.
- (39) Cabbiness, D. K.; Margerum, D. W. *J. Am. Chem. Soc.* **1969**, *91*, 6540–6541.
- (40) Cabbiness, D. K.; Margerum, D. W. *J. Am. Chem. Soc.* **1970**, *92*, 2151–2153.
- (41) Fabbriizzi, L.; Licchelli, M.; Mosca, L.; Poggi, A. *Coord. Chem. Rev.* **2010**, *254*, 1628–1636.
- (42) dos Santos, C. M. G.; Barrio Fernández, P.; Plush, S. E.; Leonard, J. P.; Gunnlaugsson, T. *Chem. Commun.* **2007**, 3389–3391.
- (43) (a) Amendola, V.; Esteban-Gomez, D.; Fabbriizzi, L.; Licchelli, M.; Monzani, E.; Sançenon, F. *Inorg. Chem.* **2005**, *44*, 8690–8698. (b) Carreira-Barral, I.; Rodríguez-Blas, T.; Platas-Iglesias, C.; de Blas, A.; Esteban-Gomez, D. *Inorg. Chem.* **2014**, *53*, 2554–2568.
- (44) Boiocchi, M.; Fabbriizzi, L.; Garolfi, M.; Licchelli, M.; Mosca, L.; Zanini, C. *Chem.—Eur. J.* **2009**, *15*, 11288–11297.
- (45) Licchelli, M.; Milani, M.; Pizzo, S.; Poggi, A.; Sacchi, D.; Boiocchi, M. *Inorg. Chim. Acta* **2012**, *384*, 210–218.
- (46) Krapcho, A. P.; Kuell, C. S. *Synth. Commun.* **1990**, *20*, 2559–2564.
- (47) He, Y.; Kou, H.-Z.; Li, Y.; Zou, B. C.; Xiong, M.; Li, Y. *Inorg. Chem. Commun.* **2003**, *6*, 38–42.
- (48) Gans, P.; Sabatini, A.; Vacca, A. *Talanta* **1996**, *43*, 1739–1753. <http://www.hyperquad.co.uk/index.htm>, accessed April 30, 2014.
- (49) Wilcox, C. S. *Frontiers in Supramolecular Chemistry and Photochemistry*; VCH: Weinheim, Germany, 1991; pp 123–143.
- (50) Wolsey, W. C. *J. Chem. Educ.* **1973**, *50*, A335–A337.
- (51) Farrugia, L. J. *J. Appl. Crystallogr.* **1999**, *32*, 837–838.
- (52) North, A. C. T.; Phillips, D. C.; Mathews, F. S. *Acta Crystallogr.* **1968**, *A24*, 351–359.
- (53) *SAINT Software Reference Manual*, version 6; Bruker AXS Inc.: Madison, WI, 2003.
- (54) Sheldrick, G. M. *SADABS Siemens Area Detector Absorption Correction Program*; University of Göttingen: Göttingen, Germany, 1996.
- (55) Altomare, A.; Burla, M. C.; Camalli, M.; Cascarano, G. L.; Giacovazzo, C.; Guagliardi, A.; Moliterni, A. G. G.; Polidori, G.; Spagna, R. *J. Appl. Crystallogr.* **1999**, *32*, 115–119.
- (56) Sheldrick, G. M. *Acta Crystallogr.* **2008**, *A64*, 112–122.
- (57) Dyer, E.; Johnson, T. B. *J. Am. Chem. Soc.* **1932**, *54*, 777–787.
- (58) McFarland, J. W.; Green, D.; Hubble, W. J. *Org. Chem.* **1970**, *35*, 702–704.
- (59) Hathaway, B. J. *Struct. Bonding (Berlin)* **1984**, *57*, 55–118.
- (60) Rosokha, S. V.; Lampeka, Y. D. *J. Chem. Soc., Dalton Trans.* **1993**, 631–636.
- (61) Kang, S.-G.; Song, J.; Jeong, J. H. *Inorg. Chim. Acta* **2004**, 357, 605–610.
- (62) Barefield, E. K. *Coord. Chem. Rev.* **2010**, *254*, 1607–1627.
- (63) Thöm, V. J.; Boeyens, J. C. A.; McDougall, G. J.; Hancock, R. D. *J. Am. Chem. Soc.* **1984**, *106*, 3198–3207.
- (64) Lever, A. B. P. *Inorganic Electronic Spectroscopy*; Elsevier: Amsterdam, The Netherlands, 1984.
- (65) Fabbriizzi, L.; Licchelli, M.; Poggi, A.; Sacchi, D.; Zampa, C. *Polyhedron* **2004**, *23*, 373–378.
- (66) Fabbriizzi, L.; Foti, F.; Licchelli, M.; Maccarini, P. M.; Sacchi, D.; Zema, M. *Chem.—Eur. J.* **2002**, *8*, 4965–4972.
- (67) Lipscombe, W. N.; Sträter, N. *Chem. Rev.* **1996**, *96*, 2375–2434.